Road Curvature Decomposition for Autonomous Guidance

Author, co-author (Do NOT enter this information. It will be pulled from participant tab in MyTechZone)

Affiliation (Do NOT enter this information. It will be pulled from participant tab in MyTechZone)

Abstract

Vehicle autonomy is critically dependent on an accurate identification and mathematical representation of road and lane geometries. Many road lane identification systems are ad hoc (e.g., machine vision and lane keeping systems) or finely-discretized path data redundant external vehicle tracking systems. A novel Midwest Discrete Curvature (MDC) method is proposed in which geodetic road data is parsed along road directions and digitally stored in a road data matrix. Road data is discretized to geospatial points and curvature and road tangent vectorization, which can be utilized to generate consistent, mathematically-defined road profiles with deterministic boundary conditions, consistent non-holonomic boundary constraints, and a smooth, differentiable path which connects critical road coordinates. The method was evaluated by discretizing three road segments: a hypothetical road consistent with AASHTO Green Book design standards, a road segment discretized using satellite photography and GPS data points, and an in-vehicle GPS trace collected at 10 Hz. Improvements and further research were recommended to expand findings, but results indicated potential for implementation into road modeling which could be the foundation of new autonomous vehicle guidance systems which are complimentary to existing autonomous systems.

Keywords: Trajectory Generation, Path Generation, Curvature, AASHTO, V2I, Vehicle-to-Infrastructure

Introduction

Motivation

Vehicle autonomy has been touted as the future of transportation, but there are significant challenges which remain to be addressed. The electronic replacement or augmentation of dynamic driving tasks performed by human drivers, such as steering, braking, and applying throttle, requires the accurate perception of the environment, potential safety risks in a decision tree, and selection of optimal outcomes [1].

Tremendous growth has been achieved in driving augmentation devices, collectively termed “Advanced Driver Assistance Systems” or ADAS [2]. Safety organizations such as the Institute for Highway Safety (IIHS), Highway Loss Data Institute (HLDI), and the National Highway Traffic Safety Administration reviewed recent U.S. traffic data and confirmed that ADAS systems directly contributed to an overall reduction in annual crashes, and likely prevented deaths and serious injuries [3][4].

However, road navigation remains the biggest hurdle for fully-autonomous vehicle implementation. Current vehicle guidance techniques have relied on one of two possible techniques: high-precision tracking using a redundant network of position tracking sensors in low-speed, urban environments; and lane edge identification using either LIDAR or machine optics. Both techniques develop an ad hoc estimation of the desired position within a lane (i.e., the lane centerline), estimate the vehicle’s current offset from that desired path, and identify what corrective factors are necessary for the vehicle’s trajectory to rejoin the desired path. Therefore, before determining what vehicle controls are necessary to follow a target path, the geometry of the target path must first be identified.

A research study conducted at the University of Nebraska-Lincoln (UNL) identified techniques for generating a highly-accurate, algorithmic road path which could be utilized within a framework of autonomous vehicle operations or as a driver assistance system. The system utilizes precisely-mapped road path coordinates, vehicle-to-roadside infrastructure (V2I) wireless communication to relay updates in road path and to assist with vehicle triangulation, and a vehicle positioning and reaction algorithm.

The objective of this paper is to describe the framework for identifying boundary conditions for highly-accurate road path descriptions, including geospatial and non-holonomic boundary conditions, and to use those boundary conditions to formulate highly-accurate mathematical representations of lane corridors. The lane paths must be smooth, differentiable, and comprised of deterministic and reproducible representations of geospatial road data.

Path Prediction in Autonomous Vehicles

In this paper, a path is defined a connection in between two points (i.e. Point A to Point B). Any curve which connects two points is therefore a possible path, as shown in Figure 1. The optimized path is identified as the path which closely follows the geometry of a lane centerline, is continuous and differentiable across segments, and minimizes mathematical instabilities or irregularities. Vehicle trajectory is defined as the path that the vehicle CG followed between two points (i.e., trace-line).

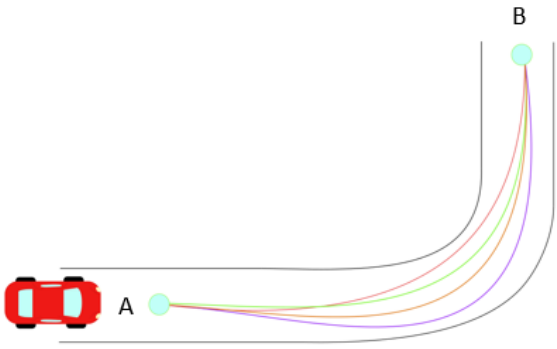

Figure 1. Different Trajectories in Path from Point A to Point B.

Human and autonomous drivers both operate the vehicle using Path Planning, which consists of the estimation of the vehicle's future trajectory given the vehicle's current position, velocity, acceleration, and operational constraints. Characteristically, optimal paths are selected based on evaluation of path intersections of traversable and non-traversable zones, as well as the evaluation of input controls required to produce the trajectory. Path planning for vehicles and robotics applications utilize physics models, geospatial curve modeling and estimation, and feedback controls [5].

Path planning applied to vehicle guidance may include sampling-based planning, which uses sampling from sensors to create a path based on limited data sets; probabilistic methods, which rely on approximating the free space available for navigation such as Probabilistic Road Maps and Rapidly Exploring Random Trees [5][6]; and Phase Space Planning which incorporates different sampling-based planning algorithms and compares them to extract the most optimal one [6].

All currently-implemented Path Planning algorithms for autonomous vehicle controls rely on narrow sample spacing to limit error. Path Planning formulations are either ad hoc (e.g., LIDAR, machine vision) or driven by low-speed, continuously-monitored GNSS triangulation with external ground-based monitoring compared to a highly-discretized road coordinate map. Vehicle sensors are also used generate navigational maps, for example discretizing areas of space from an image to determine if they are feasible for navigation.

During on-road driving, parameters such as velocity, acceleration dictate which possible paths may result in feasible trajectories. Path descriptions have been described using variational methods, clothoids, and velocity profiles [7] [8] [9]. Variational methods arise from optimizing functionals with non-holonomic constraints (i.e. constraints on the velocity and acceleration) [10]. These methods yield polynomial solutions of high order that are treated as boundary value problems (BVP) during vehicle navigation [11] [12]. Clothoid functions (Cornu Spirals or Euler Spiral), and spline functions are also studied in autonomous research because of their effectiveness to connect a straight line with a constant radius curve [13] [14] [15].

These trajectory estimates are then combined with optimization theory to be implemented into controllers for navigation purposes [16]. In general, these trajectories focus on providing a continuous function (up to the third derivative) while being smooth (i.e. minimizing the jerk $\frac{d^3x}{dt^3}$) [17] [18]. Alternative trajectory estimates

Method Formulation

Vehicle Dynamics and Road Design

Researchers utilized principles of vehicle dynamics in order to generate a road mapping technique which would automatically resolve limitations on vehicle stability and control. It was noted that all vehicle-road interactions are governed by the force generated at the wheels, and all vehicle controls are dictated by the direction and magnitude of friction force [19] [20]. Using Newton's 2nd Law, those forces can be related to the fundamental kinematic constraints of path motion.

A Frenet-Serret reference frame is used along with unit vectors of N (normal), T (tangential), and B (binormal, out of plane) as shown in Figure 2. For this paper, it is assumed that the vehicle navigates on a 2D Euclidean Space.

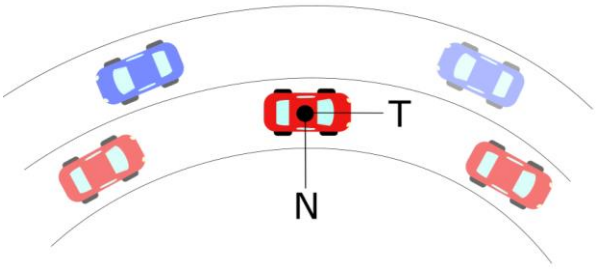

Figure 2. Normal-Tangential Coordinates Example in Vehicle's Center of Mass.

The net acceleration acting on the vehicle at an instant in time is described by the time variance of the path. These limits are related to the acceleration a vehicle goes under circular motion, which is denoted as:

$$a = \dot{v}\,T + \kappa v^2\,N$$

Where:

a = Total Acceleration of Vehicle (m/s^2)

v = Tangential Velocity of Vehicle (m/s)

κ = Curvature at an Instantaneous Point (m^{-1})

N =Normal Unit Vector

T= Tangential Unit Vector

Longitudinal accelerations are produced by a net longitudinal force, which either increases or decreases vehicle speed. Lateral accelerations in the normal direction (perpendicular to the velocity vector) do not affect speed and instead turn the vehicle's trajectory. Lateral forces are generated during turns and from road cross-section geometry (superelevation, banks, crowning). Curvature, κ, which is the reciprocal of the radius of curvature, is related to the instantaneous rate of change of the tangential unit vector T with respect to time or distance traveled [21][22][23].

In recognition of measurable data on the vehicle and vehicle dynamics constraints, the American Association of State Highway and Transportation Officials (AASHTO) standardized road designs which control for tire-pavement friction using equations for superelevation,

crowning, and turn radius [24]. These road design parameters are based on numerous historical studies of driver tolerance for lateral accelerations [25]. Speed limits are controlled on roadways based on measured reductions in friction during wet travel conditions [26]. Hence, the Frenet-Serret coordinates are highly compatible with onboard vehicle systems and prevailing road geometrical design.

Moreover, determining target vehicle path geometries using Frenet-Serret formulation is highly conducive for autonomous vehicle control systems. For example, accelerometers measure acceleration along principal axes; rate transducers record vehicle angular rates of change; gyroscopes identify instantaneous vehicle inclinations; wheel sensors and GPS are useful for estimating current speeds; and steering wheel rotational sensors can detect wheel steer angles. Wheel steer angles can be related to the instantaneous curvature using Ackerman estimates and corrections for understeer gradient [19] [20]. For vehicles whose orientation closely follows the roadway tangent vector *T*, the lateral acceleration can provide an additional evaluation of the instantaneous curvature of the vehicle.

Researchers developed target path geometry constraints using Frenet-Serret coordinates in local space and then mapped those coordinates to the surface of the earth using transformation matrices based on GPS coordinates. Thus, curvature can be expressed in a vector form that has a direction parallel to the Normal Unit Vector shown in Figure 2. Similarly, a vector perpendicular to the curvature direction will provide a velocity tangent vector approximation at that point. This velocity vector provides a heading angle to the desired trajectory that is needed to follow a road path. Researchers therefore generated mathematical relationships to identify the non-holonomic constraints which aligned with Frenet Serret formulation using discrete geospatial point data.

Spatial Curvature Formulation

The instantaneous curvature of a geospatial point (deemed "A") was obtained using the spatial coordinates of adjacent points. The technique may be scaled with smaller or larger segmentation, leading to an optimized computational cost, *O(n)* [27].

Let a scalene triangle with corners A, B, C have a circumscribed circle of radius ρ in Euclidean 2D space as shown in Figure 3. The vertices of the triangle are connected using vectors *AB*, *AC*, and *BC*.

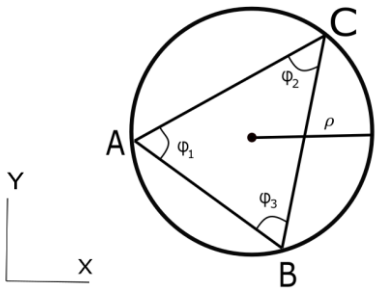

Figure 3. Circumscribed Circle in Scalene Triangle.

A vector *AD*, equal to the cross product in between the vectors *AB* and *AC*, will be normal to the plane defined by the intersection of *AB* and *AC*. The magnitude for vector *AD* may be identified based on the cross product:

$$\|D\| = \|AB \times AC\| = \|AB\| \, \|AC\| \, \sin\phi_1$$

Let a vector *E* be the cross product of *AD* with the vector *AB*. defining this new vector in the direction of e as shown in red in Figure 4. The magnitude of vector *E* is defined as:

$$\|E\| = \|D \times AB\| = \|AB\|^2 \|AC\| \, \sin\phi_1$$

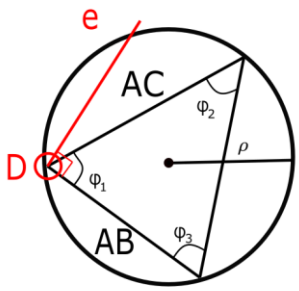

Figure 4. First Unit Vector Direction on Triangle.

Similarly, let a vector *F* be the cross product of *AD* with the vector *AC*, defining this new vector in the direction of f shown in blue in Figure 5. The magnitude of vector *f* is defined as:

$$\|F\| = \|D \times AC\| = \|AB\| \|AC\|^2 \, \sin\phi_1$$

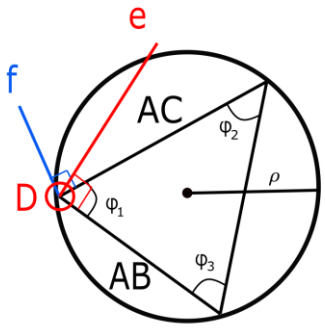

Figure 5. First- and Second-Unit Vectors on Triangle.

The unit vectors of e and f are defined by the following:

$$e = \frac{E}{\|AB\|^2 \|AC\| \sin\phi_1}$$

$$f = \frac{F}{\|AB\| \|AC\|^2 \sin\phi_1}$$

The midsection of any triangle's side intersects with each other at a point P corresponding to the center of the circle inscribing points A, B, and C. These intersecting lines denote two triangles with the same angle ϕ_1 in between the unit vectors and their corresponding midsections as shown in Figure 6.

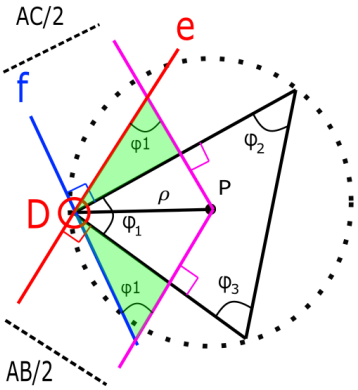

Figure 6. Radius of Curvature obtained from Geometric Relationships.

From these triangles, the radial vector *AP* may be described using components along unit vectors e and f. As a result, vector *AP* is described as:

$$AP_1 = \frac{AC}{2\sin\phi_1}\ e = \frac{E}{2\|AB\|^2\sin^2\phi_1}$$

$$AP_2 = \frac{-AB}{2\sin\phi_1}\ f = \frac{-F}{2\|AC\|^2\sin^2\phi_1}$$

From our previous definition of the vector *AD*, it is possible to simplify further:

$$AP_1 = \frac{\|AC\|^2 E}{2\|D\|^2}$$

$$AP_2 = \frac{-\|AB\|^2 F}{2\|D\|^2}$$

With these components, it is possible to obtain the magnitude as follows:

$$AP = \frac{\|AC\|^2 E}{2\|D\|^2} - \frac{\|AB\|^2 F}{2\|D\|^2}$$

$$\rho = \frac{\|AC\|^2 E - \|AB\|^2 F}{2\|D\|^2}$$

Using previous definitions of *E* and *F*:

$$\rho = \frac{\|AC\|^2\|AD\times AB\| - \|AB\|^2\|AD\times AC\|}{2\|D\|^2}$$

Using previous definition of *AD*, it is possible to obtain the radius of the prescribed circle in terms of only the difference in between points A, B and C.

$$\rho = \frac{\|AC\|^2\|(AB\times AC)\times AB\| - \|AB\|^2\|(AB\times AC)\times AC\|}{2\|(AB\times AC)\|^2} \quad (1)$$

Noting that $\kappa = {}^1/_{\rho}$, it is possible to calculate curvature as:

$$\kappa = \frac{2\|(AB\times AC)\|^2}{\|AC\|^2\|(AB\times AC)\times AB\| - \|AB\|^2\|(AB\times AC)\times AC\|} \quad (2)$$

This process can be executed for small and large spacing between consecutive points along a curve, as shown in Figure 7. As a result, both finely-sampled and coarsely-sampled data may be utilized to generate geospatial curvature maps.

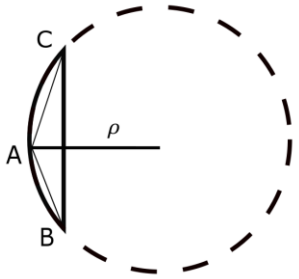

Figure 7. Scalene Triangle in Small Arc-Segment.

Curvature is related to the second-order differential of position and has strong association with the limits on lateral acceleration. Given that the 2nd order differential equations are used to condition non-holonomic boundary conditions, determination of instantaneous curvature provides half of the data needed to fully define smooth, continuous, and deterministic target path formulations.

In addition to the 2nd order curvature-based non-holonomic constraint, a 1st-order boundary condition was also identified based on the roadway tangent vector. The roadway tangent vector, *T*, is determined using an orthogonal phase shift of the curvature vector, such that:

$$T = \frac{(AD\times\kappa)}{\|(AD\times\kappa)\|} \quad (3)$$

Imposing local curvature and tangent coordinate vectors at each geospatial road data-point ensures that the target road path will be consistent with Frenet-Serret formulation. Then, roadway data checking can be performed to ensure that the curvature and point data is consistent with road design parameters and useful for identifying potential errors or skew datasets.

Segment Length Estimation

Between each consecutive set of geospatial points, the optimized roadway target path length, *s*, may be known to assist with relating vehicle current position to an equivalent position along the roadway target path. This error calculation is essential for determining if the vehicle's trajectory angle, speed, and current position combination put the vehicle at risk of departing the lane or roadway.

The length of each segment of the road path may be identified using the fundamental determination of arc length to radius based on included angle. The arc-length s of a curve is defined as the length traveled by the angle θ along a constant radius ρ:

$$\theta = \frac{s}{\rho}$$

Recalling curvature is the inverse of the radius of curvature, it follows that:

$$\theta = \kappa s$$

A differential form may be used to relate the change in angle to the segment length, *s*:

$$ds = \frac{d\theta}{\kappa}$$

By separation of variables and integration:

$$\int ds = \int \frac{d\theta}{\kappa}$$

Finally, the segment lengths can be determined can be found through numerical integration of the curvature and angle changes:

$$\Delta s = \int \frac{d\theta}{\kappa} \tag{4}$$

Road Curvature Decomposition

The curvature formulation shown in Equation (2) and road segment calculations shown in Equation (4) may be applied to a discrete point cloud collected from a road geometry to determine the instantaneous curvature for every point, except at terminal ends of roadways. An example of the determination of curvature is shown in Figure 8.

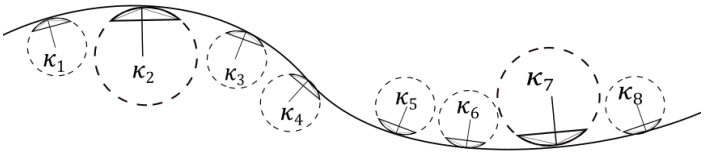

Figure 8. Road with Discrete Curvature Sections

When roadway curvature is tangent, the curvature evaluates to zero and is stable; in contrast, the instantaneous radius of curvature of a tangent road is infinite for a 2D Cartesian map, or may be related to the earth radius in 3D maps. An example of the radius vector map is shown in Figure 9.

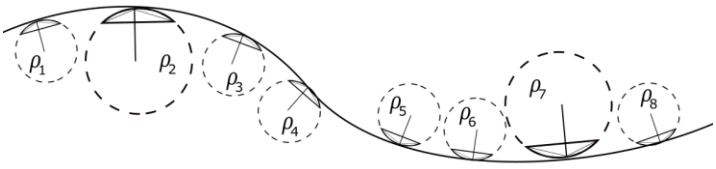

Figure 9. Road with Discrete Radius of Curvature Sections

With the use of different technologies such as Aerial Photography, LIDAR scanning, GPS collection, or Road Surveying, it is possible to obtain a geospatial map of roadway centerlines or roadway lane edges (or limits of travelway for rural, unmarked roads). This data may be processed to identify the instantaneous curvature and heading angle of road points, and the segment length connecting consecutive points on the roadway. Continuous mathematical curve formulations may then be used to connect the geospatial point data in accordance with the curvature and heading angle calculations calculated previously. An example of this technique would be a parametric polynomial representation for X and Y road coordinates. An example of the road curvature decomposition scheme is represented in Figure 10.

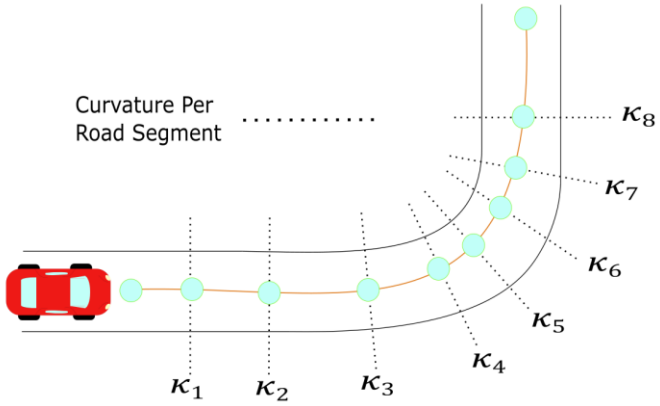

Figure 10. Road Curvature Decomposition Example

Using the discrete curvatures calculated for each point, a piecewise-linear, continuous curvature model was developed. Road profiles may be deterministically modeled using relationships for curvature points, heading angles, and roadway segment lengths. Application of this technique to the creation of target paths was deemed the "Midwest Discrete Curvature" (MDC) method. The efficacy of this method in estimating road profiles was evaluated in the following sections.

Implementations

Typical highway roads are designed based on AASHTO guidelines to provide a natural, easy-to-follow path for drivers, such that the lateral accelerations increase and decrease gradually as the vehicle begins and ends curved road segments [24]. The continuity of the road curvature and adaptability for road tangents using the MDC method were compared by calculating the curvature throughout a road segment constructed consistently with AASHTO design guidelines, then compared using real-world data from satellite photography and point selection as well as GPS data.

AASHTO Base Model

This model consisted on strictly using AASHTO guidelines to design an ideal highway road for a vehicle traversing at constant 60 mph. The curve consisted of 5 different sections that can be classified as: straight section, entrance transition, constant radius curve, exit transition and straight section. The road path constructed in accordance with AASHTO Green Book design guidelines is shown schematically in Figure 11.

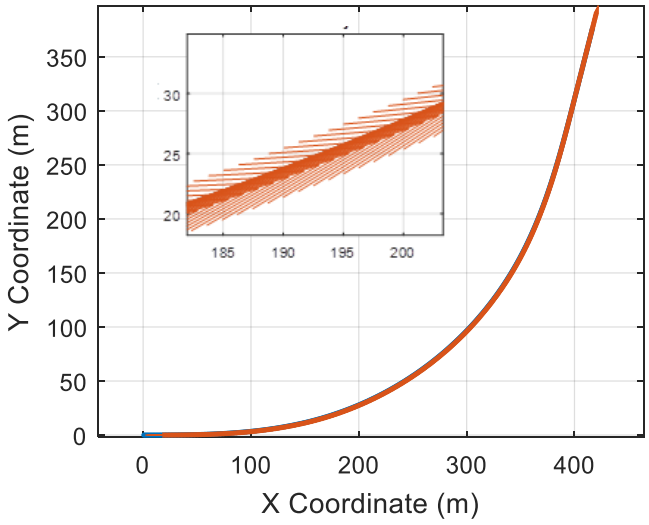

Figure 11. Finely-Discretized AASHTO Base Model: Road with Velocity Vectors.

Applying the MDC approach to this curve, curvature vectors were plotted with respect to the road segments as shown Figure 12. The curvature magnitude was plotted with respect to road segments to obtain a base curvature profile as shown in Figure 13.

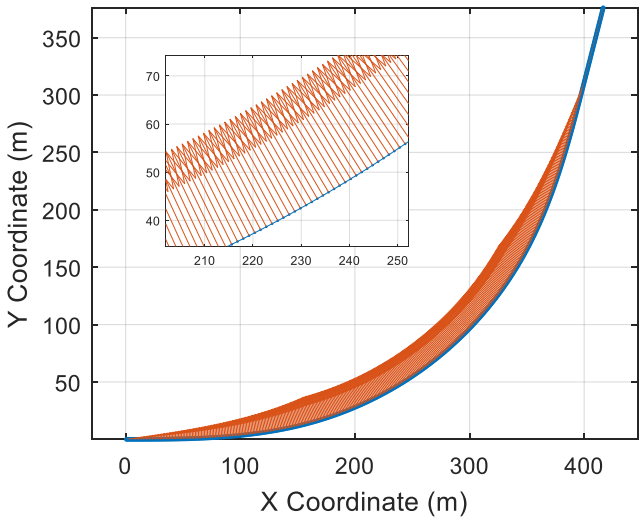

Figure 12. Finely-Discretized AASHTO Base Model: Road with Curvature Vectors.

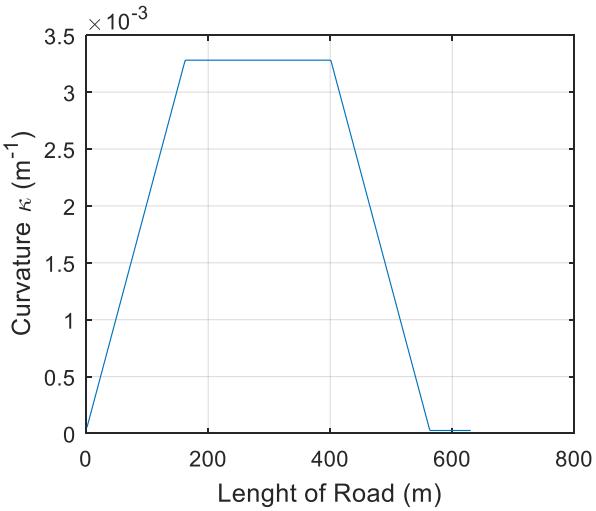

Figure 13. Finely-Discretized AASHTO Base Model: Curvature κ vs. Cumulative Curve Length.

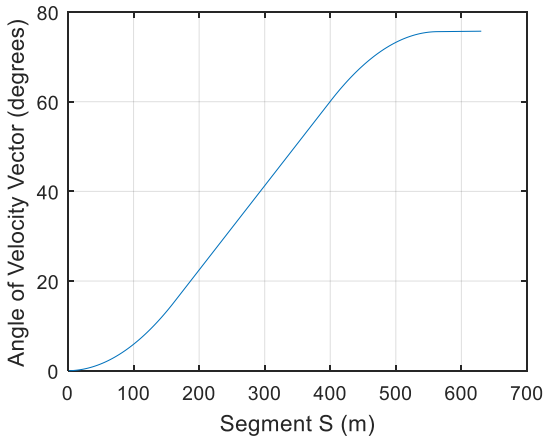

Figure 14. Finely-Discretized AASHTO Base Model: Orthogonal Phase Shift of Curvature Vector to Calculate Tangent Vectors.

Roadway Decomposition: Google Earth Images

Next, researchers evaluated the efficacy of the continuous curvature model using finely-discretized data collected from aerial photography of a real road segment with a design speed of 60 mph. The road is located in I-80 connecting Lincoln and Omaha in Nebraska as shown in Figure 15. The points were picked as close as possible to resemble the road centerline of the highway. The road profile and resulting vectors from applying the discrete geometry approach are shown in Figure 16. It is noticeable that the fine discretization of the road points led to some inconsistencies between consecutive tangent vectors. The curvature magnitude with respect to length was also plotted in Figure 17 and it was observed that magnitude deviations also increased considerably compared to the AASHTO Green Book theoretical road design model. However, these inconsistencies are strongly related to very short segment lengths relative to curve radii. By using longer segment lengths or averages spanning multiple longitudinal points, results are considerably smoother.

Figure 15. Google Earth: I-80 Road Example

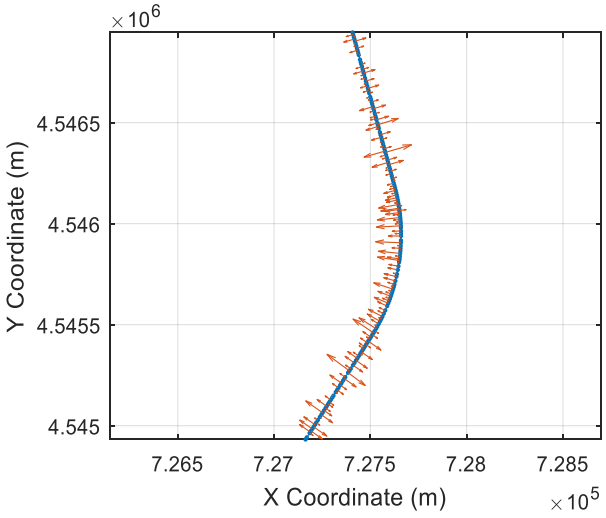

Figure 16. Google Earth Model: Road with Curvture Vectors.

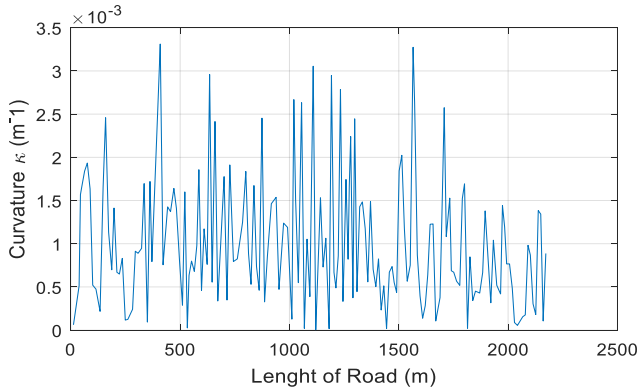

Figure 17. Google Earth Model: Curvature κ vs. Cumulative Curve Length.

Although curvature magnitudes varied significantly due to short segment lengths, the velocity vector angles were observed to be smooth overall along the segments as shown in Figure 18.

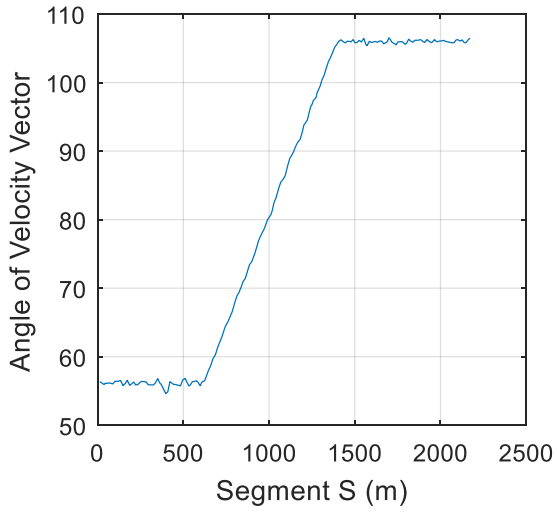

Figure 18. Google Earth Model: Orthogonal Phase Shift Approach.

Despite noise in the segmented curvature and heading angle discretization, the resulting plot of estimated lane centerline matched the road profile with excellent accuracy. An overplot of the calculated road profile based on the MDC method is shown in Figure 19.

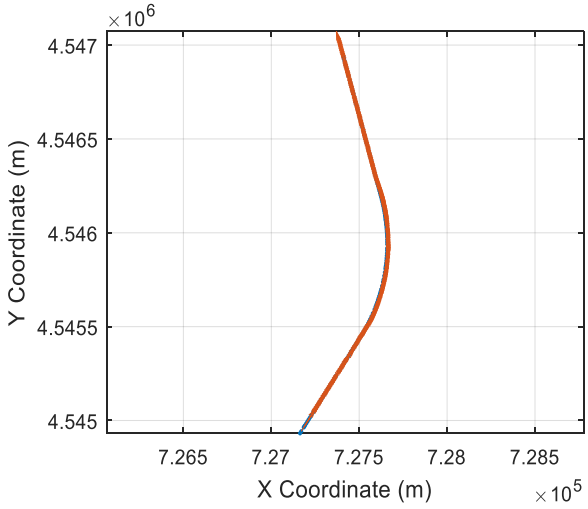

Figure 19. Google Earth Model: Road with Tangent Vectors.

GPS Model

The last evaluation of the value of the MDC method utilized GPS data collected while driving along a road with speed limit of 60 mph. The data was collected with a VC4000 Unit produced by Vericom Computers, Inc, at a frequency rate of 10 Hz. It should be noted that using single-trip GPS data with L1-rated accuracy provides a nominal error estimate of 1.981 m per data point [28], and therefore was the least accurate and smallest dataset evaluated. Nonetheless, applying the MDC method to identify the lane centerline coordinates demonstrated the power of this method in modeling road geometries, as shown in Figure 20, Figure 21, and Figure 22. It is expected that with larger datasets from multiple vehicle trips, highly-precise lane centerline data may be identified even using GPS without differential accuracy estimates.

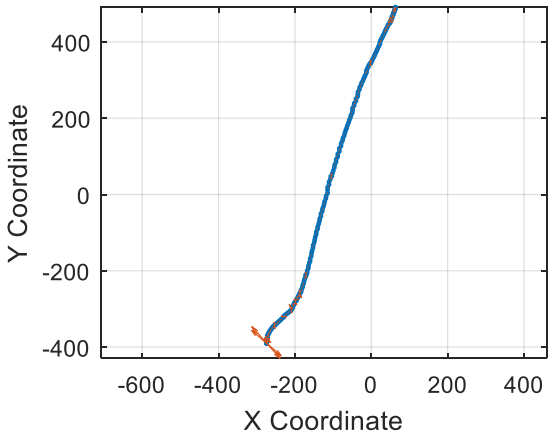

Figure 20. GPS Model: Road with Curvature Vectors.

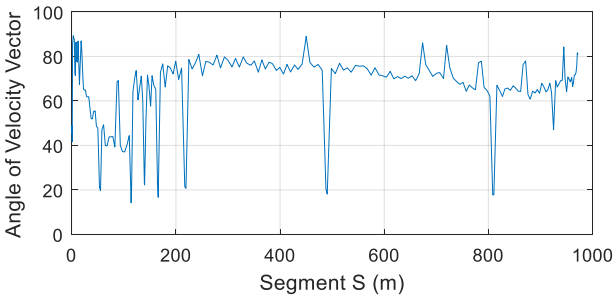

Figure 21. GPS Data: Tangent Vector Evaluation using Orthogonal Phase Shift Approach.

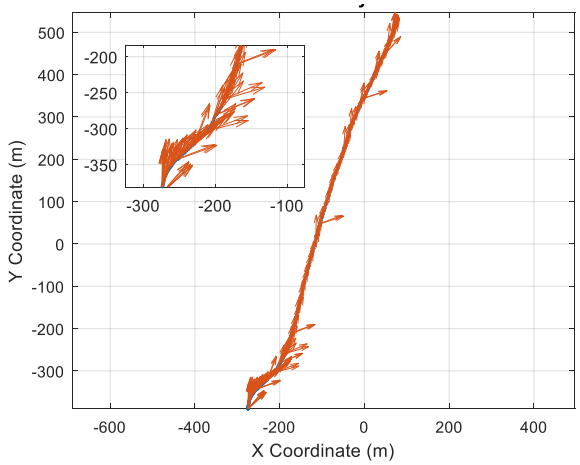

Figure 22. GPS Model: Road Construction with Tangent Vectors.

Smoothing Techniques

On trajectory generation, many techniques focus on interpolation restrict the motion of vehicles to maintain certain level of commodity and stability [29] [30]. Given that the approach presented obtains heading angle based on discrete data sets for later storage, smoothing techniques may be required to sustain a better approximation of road centerlines while offering a different option to store road decompositions.

Many methods such as Lagrange's interpolation, and Linear Regressions are used in fitting data for analysis [31]. However, for this application, a local regression with weighted linear least squares was selected to maintain a minimum contribution of the data outliers. This avoids misrepresentation of data often provided by GPS sampling as shown in Figure 21 as peaks.

The data was given a span of 15% for outlier acceptance, and the resulting smoothed GPS data is shown in Figure 23, in which outliers are not part of the desired prescribed angle values. Smoothed data was plotted and compared to original GPS model in Figure 24. It is noticeable how the data is easily smoothed from a GPS receiver. However, there is an initial swerving behavior on the heading data which could be due to initialization of the GPS.

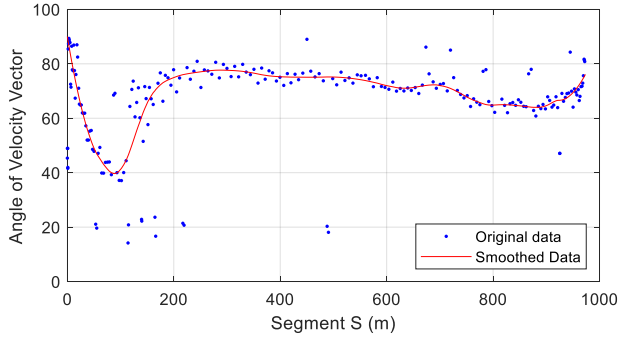

Figure 23. GPS Data: Smoothed Tangent Vector Data

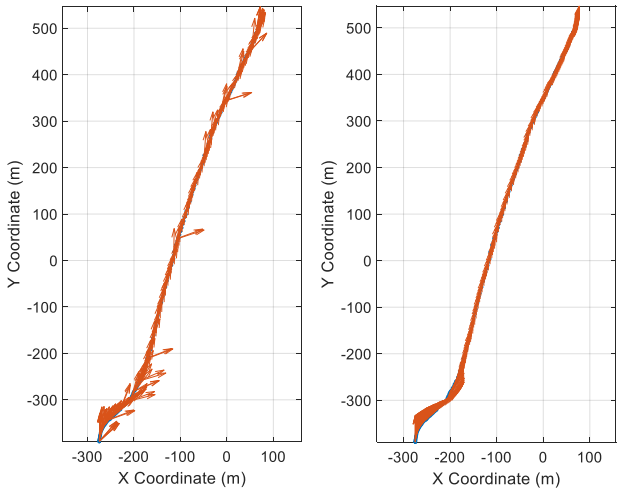

Figure 24. GPS Model: Original Data (Left) and Smoothed Data (Right)

Discussion

Road sampling data is critical for the use of the MDC method for identifying non-holonomic boundary constraints on target road paths.

Aerial data and LIDAR or survey data are two methods discussed herein.

Aerial or Satellite Photography

Similar to Google Earth, this method requires identification (either manually or through software) of the lane. This method may be easily integrated into machine learning applications to preselect estimated road geometries without manual selection. The principal disadvantage from this method is susceptibility to error around unclear lane markings, such as adjacent to heavy tree foliage, road segments under construction, or roads affected by environmental effects. Furthermore, care must be taken to identify changes to the road network caused by road construction including additional lanes or closed lanes.

Survey, LIDAR, or Photogrammetry Point Clouds

If road geometries are surveyed using conventional survey equipment or through LIDAR sampling, very high-precision lane geometries may be identified. Nonetheless the process of point selection and the narrow spacing between consecutive lane edge points may introduce considerable numerical noise. This noise may be augmented by other vehicles or visual obstructions which interfere with clear lane edge identification.

Discussion/Recommendations

The study presented has the potential to be implemented in a distributed model of vehicle automization, but is not limited solely to passenger vehicles. Examples of other vehicle types which could utilize the target path formulation for positional error estimation and corrections include agricultural vehicles, transport vehicles (e.g., autonomous trucks), unmanned aerial systems, or mobile robots.

To achieve this goal, the following scheme is proposed for an implementation of the discrete road decomposition as shown Figure 25. The first step involves collection of road data through any convenient means: GPS Data, Surveying, or Aerial Scanning. This road data contains a representation of the road centerlines which can be exported in different formats. These road centerlines are decomposed with the proposed method, stored in a road target path matrix, and transmitted wirelessly to a vehicle in motion. The infrastructure may also assist with precise vehicle localization to improve error estimation, allowing the vehicle onboard systems to have excellent real-time observation of potential deviations from the target path. Finally, a controller is developed to consider the heading based from the discrete road decomposition and navigate safely through the road.

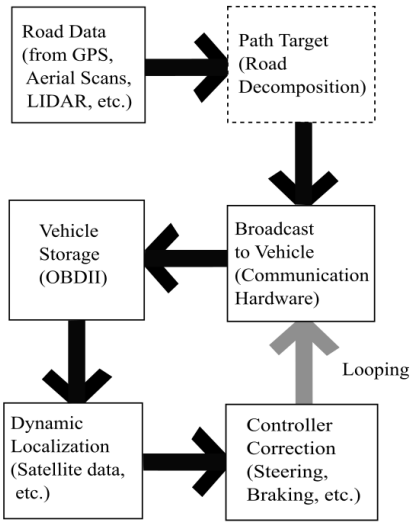

Figure 25. Implementation Scheme for Road Curvature Decomposition

Because the system does not rely on local ad hoc determination of lane boundaries, and does not utilize machine vision or de facto external tracking systems, the system is well-positioned to provide guidance system for autonomous vehicles even in adverse weather conditions, poor visibility, and even for temporary road or lane closures. The dynamic road network relay to autonomous vehicles may allow for alternative route selection in the event of congestion or crash events, and external guidance information such as tire-pavement friction reductions reported by other vehicles or estimated from weather reports may also be broadcast to the vehicle in targeted geospatial areas. As such, this technique for vehicle guidance systems could be complimentary to existing lane keeping and ADAS systems for crash avoidance or mitigation.

Research is ongoing at the University of Nebraska-Lincoln confirm the accuracy of this technique and the applicability to autonomous vehicle guidance systems. More research including empirical testing and simulation are recommended to integrate the MDC method into a broader vehicle guidance paradigm.

Summary/Conclusions

In conclusion, a method was proposed to calculate trajectories based on discrete curvature and road tangent calculations. The proposed method is consistent with AASHTO design guidelines and can be made to be compatible with vehicle performance limits by controlling allowable speed based on geospatial road curvature. Additional research was recommended to consider smoothing techniques such as Akima interpolation to provide the highest level of reliability for onboard driving, and should be verified using empirical testing and computer simulation. Successful implementation of this method could offer a new key piece to solve the autonomous vehicle paradigm under weather disruptions and/or other navigation technologies.

References

1. Stolle, C., Jacome, R., and Sweigard, M., "Autonomous Technology, A Review - MATC Year One Report", Internal Report, 2018.
2. Huetter, John. "IIHS: HLDI Estimates 24% of Fleet Had Backup Cameras, 17% Had Parking Sensors in 2016." *Repairer Driven News* (blog), February 2, 2018. https://www.repairerdrivennews.com/2018/02/02/iihs-hldi-estimates-24-of-fleet-had-backup-cameras-17-had-parking-sensors-in-2016/.
3. HLDI Bulletin, "Compendium of HLDI collision avoidance research" vol. 35, No. 34: September 2018.
4. Benson, A.J., Tefft, B.C., Svancara, A.M., & Horrey, W.J. (2018). Potential Reductions in Crashes, Injuries, and Deaths from Large-Scale Deployment of Advanced Driver Assistance Systems (Research Brief). Washington, D.C.: AAA Foundation for Traffic Safety.
5. LaValle, Steven M. "Planning Algorithms," 2006. https://doi.org/10.1017/cbo9780511546877.
6. Heinrich, S., "Planning Universal On-Road Driving Strategies for Automated Vehicles," AutoUni – Schriftenreihe. Springer, 2018. https://doi.org/10.1007/978-3-658-21954-3.
7. Kelly, A., and Nagy, B., "Reactive Nonholonomic Trajectory Generation via Parametric Optimal Control." I. J. Robotics Res. 22 (2003): 583–602. https://doi.org/10.1177/02783649030227008.
8. Dubins, L. E., "On Curves of Minimal Length with a Constraint on Average Curvature, and with Prescribed Initial and Terminal Positions and Tangents," American Journal of Mathematics 79, no. 3 (1957): 497–516. https://doi.org/10.2307/2372560.
9. Ziegler, J., Bender, P., Dang, T., and Stiller, C., "Trajectory Planning for Bertha — A Local, Continuous Method." In 2014 IEEE Intelligent Vehicles Symposium Proceedings, 450–57, 2014. https://doi.org/10.1109/IVS.2014.6856581.
10. Fox, C., "An Introduction to the Calculus of Variations. Courier Corporation," 1987.
11. Takahashi, A., Hongo, T., Ninomiya, Y., and Sugimoto, G., "Local Path Planning And Motion Control For AGV In Positioning." In Proceedings. IEEE/RSJ International Workshop on Intelligent Robots and Systems '. (IROS '89) 'The Autonomous Mobile Robots and Its Applications, 392–97, 1989. https://doi.org/10.1109/IROS.1989.637936.
12. Piazzi, A., and C. Guarino Lo Bianco. "Quintic G2-Splines for Trajectory Planning of Autonomous Vehicles." In Proceedings of the IEEE Intelligent Vehicles Symposium 2000 (Cat. No.00TH8511), 198–203, 2000.
13. Sun, Y., Zhan, Z., Fang, Y., Zheng, L. et al., "A Dynamic Local Trajectory Planning and Tracking Method for UGV Based on Optimal Algorithm," 2019-01–0871, 2019. https://doi.org/10.4271/2019-01-0871.
14. Wilde, D., "Computing Clothoid-Arc Segments for Trajectory Generation," In 2009 IEEE/RSJ International Conference on Intelligent Robots and Systems, 2440–45, 2009. https://doi.org/10.1109/IROS.2009.5354700.
15. Delingette, H., M. Hebert, and K. Ikeuchi. "Trajectory Generation with Curvature Constraint Based on Energy Minimization." In Proceedings IROS '91:IEEE/RSJ International Workshop on Intelligent Robots and Systems '91, 206–11 vol.1, 1991. https://doi.org/10.1109/IROS.1991.174451.
16. Werling, M., Ziegler, J., Soren, K., and Thrun, S., "Optimal Trajectory Generation for Dynamic Street Scenarios in a Frenet Frame," In 2010 IEEE International Conference on Robotics and Automation, 987–93. Anchorage, AK: IEEE, 2010. https://doi.org/10.1109/ROBOT.2010.5509799.
17. Werling, M., Kammel, S., Ziegler, J., Groll, L., "Optimal Trajectories for Time-Critical Street Scenarios Using Discretized Terminal Manifolds." The International Journal of Robotics Research 31, no. 3 (March 2012): 346–59. https://doi.org/10.1177/0278364911423042.
18. Sun, Y., Zhan, Z., Fang, Y., Zheng, L. et al., "A Dynamic Local Trajectory Planning and Tracking Method for UGV Based on Optimal Algorithm," 2019-01–0871, 2019. https://doi.org/10.4271/2019-01-0871.
19. Gillespie, T. D. "Fundamentals of Vehicle Dynamics," SAE Int. ISBN 1-56091-199-9, 1992.
20. Pacejka, H. B. Tyre and Vehicle Dynamics. Butterworth-Heinemann, 2006.
21. Carmo, Manfredo P. Do. Differential Geometry of Curves and Surfaces. 1 edition. Englewood Cliffs, N.J: Prentice-Hall, 1976.
22. Pressley, A. N. Elementary Differential Geometry. 2nd ed. Springer Undergraduate Mathematics Series. London: Springer-Verlag, 2010. https://doi.org/10.1007/978-1-84882-891-9.
23. O'Reilly, Oliver M. Engineering Dynamics: A Primer. Springer Science & Business Media, 2010.
24. A Policy on Geometric Design of Highways and Streets, (The Green Book) 6th Edition. American Association of State Highway, 2011.
25. Morral, J. F., and Talarico, R. J., "Side Friction Demanded and Margin of Safety on Horizontal Curves," Journal of the Transportation Research Board, 1994, pp. 145-152.
26. Henry, J. J. "Evaluation of Pavement Friction Characteristics, a Synthesis of Highway Practice." 2000, NCHRP Synthesis 291, 7p.
27. Are Mjaavatten (2019). Curvature of a 2D or 3D curve (https://www.mathworks.com/matlabcentral/fileexchange/69452-curvature-of-a-2d-or-3d-curve), MATLAB Central File Exchange. Retrieved May 24, 2019.
28. William J. Hughes Technical Center, "Global Positioning System (GPS) Standard Positioning Service (SPS) Performance Analysis Report," Federal Aviation Administration, 2017.
29. Levien, R. L., "From Spiral to Spline: Optimal Techniques in Interactive Curve Design," n.d., 191.
30. Akima, H. "A New Method of Interpolation and Smooth Curve Fitting based on Local Procedures," J. ACM 17, no. 4 (October 1970): 589–602. https://doi.org/10.1145/321607.321609.
31. Heath, Michael T. Scientific Computing: An Introductory Survey, Revised Second Edition. SIAM, 2018.

Contact Information

Dr. Cody Stolle, Midwest Roadside Safety Facility, 2200 Vine St, Lincoln, NE 68503, Phone: (402) 472-4233, E-mail: cstolle2@unl.edu

Ricardo Jacome, Midwest Roadside Safety Facility, 2200 Vine St, Lincoln, NE 68503, E-mail: rjacome@huskers.unl.edu

Michael Sweigard, Midwest Roadside Safety Facility, 2200 Vine St, Lincoln, NE 68503, E-mail: mikesweigard@huskers.unl.edu

Acknowledgments

The research described in this paper is funded, by the Mid-America Transportation Center via a grant from the U.S. Department of Transportation's University Transportation Centers Program, and this support is gratefully acknowledged. The contents reflect the views of the authors, who are responsible for the facts and the accuracy of the information presented herein, and are not necessarily representative of the sponsoring agencies.